XLI CILAMCE
XLI Ibero-Latin American Congress on Computational Methods in Engineering
16-19 November, 2020 FOZ DO IGUAÇU PARANÁ - BRAZIL

The nonlinear modal analysis of a barge-type offshore wind turbine

Elvidio. Gavassoni[1], Paulo D. G. Zwierzikowski [1]

[1]*Prog. de Pós-Graduação em Eng. Constr. Civil, Universidade Federal do Paraná*
DCC/TC, Bloco III Caixa Postal 19011, 81531-980
gavassoni@ufpr.br, paulognatta@gmail.com

Abstract. Wind turbine use is increasing all over the world. At depth-water greater than 50 m floating support platforms will be the most economical type of support structure to use. Among the numerous floating support-platform configurations possible for the use with offshore wind turbines one may cites the barge, whose static stability in pitch and roll is achieved using a large waterplane area. Such structures can exhibit large displacements when vibrating. This scenario demands a nonlinear dynamic analysis of the problem. The main goal of this study is to use reduced order models, based on the nonlinear normal modes, to identify and to analyze the nonlinear dynamic behavior of a reference turbine of 5 MW supported by a barge floating structure. Free and forced vibrations are studied. The existence of multiple solutions, unstable solutions and bifurcations are detected. The use of the Mathieu's chart allows the study of the stability of the solutions. The results show that the nonlinear normal modes are an efficient tool to capture some important behavior and to perform fast parametrical studies. The reduced order model results are compared to the numerical integration of the equations of motion and a good agreement between both results is found.

Keywords: nonlinear normal modes, floating wind turbine, dynamic response, Mathieu chart.

1 Introduction

Offshore wind energy exploitation has been growing fast in the last years (Ohlenforst et al., [1]). The advancing of deployment of wind farms at deep sea conditions leads to an increasing in the use of floating offshore wind turbines (FWOT). As an example of floating platforms, the barge-type achieves basic static stability in pitch and roll using a large waterplane area and shallow draft. Wind towers are the largest rotating structures on earth (Sarkar and Fitzgerald, [2]) and are fabricated using materials with very large specific strength (Zuo et al.,[3]), resulting in very slender structures. These features combined to the harsh ocean environmental conditions leads to large amplitude vibrations and a nonlinear dynamic analysis is mandatory for a safe design of those structures. The use of models with a large number of degrees-of-freedom such as element finite schemes could be a very cumbersome task due, mainly in parametric analysis. An alternative to overcome such difficulties is to use the nonlinear normal modes (NNMs) concept to obtain reduced order models of the problem (Gavassoni et al., [4]).

This work uses the nonlinear normal modes to derive a reduced order model of a wind turbine supported by an ITI Energy Barge 40 m x 40 m x 10 m barge with eight catenary mooring lines (Jonkman [5]). The Lagrange formulation is used to derive the nonlinear equations of motion of the FWOT. The reduced order model (ROM) obtained by the use of the NNMs are used to study the free and forced vibrations of the problem. ROM based results are compared to the numerical integration of the equations of motions. The stability of the solutions is investigated using Mathieu's chart. Some rich nonlinear dynamics phenomena are found such as multiple periodic solutions, limit cycles, node-saddle bifurcations, unstable solutions, jump and dynamic hysteresis.

2 Formulation

The dynamic model used here consists of a National Renewable Energy Laboratory (NREL) 5-MW wind turbine, completely described by Jonkman and coworkers [6], supported by an ITI Energy barge floating platform whose description is given by Jonkman [5]. The barge-tower structure is modelled here following the work of He et al. [7] which have used a two time (t) dependent degrees-of-freedom rigid body system in terms of the barge pitch motion (θ_B) and the tower fore-aft motion (θ_T). The tower is modelled as a rigid beam with a single lumped mass (m_T) (considering the tower, nacelle and blades masses together) located at its center of mass distant L_T from the hinged point O. The tower-barge connection stiffness is modelled as a linear rotational spring of constant equal to k_T. The barge mass, m_B, is located at a distance L_B from the hinged point O. The restoring moments, given by mooring systems and buoyance, are modelled using a linear rotational spring of constant equal to k_B.

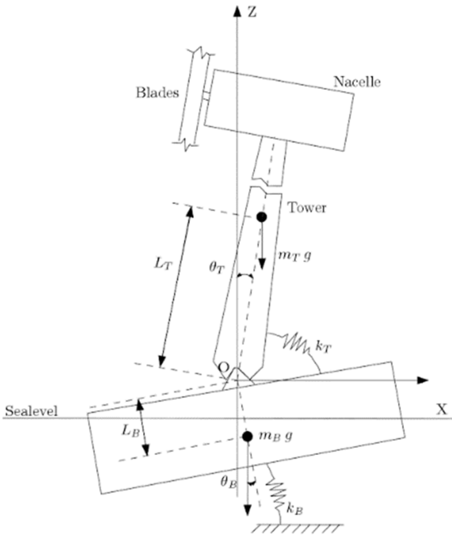

Figure 1. Rigid body model

Table 1. FWOT parameters (Jonkman, [5] ; He et al. [7])

Parameter	Value	Unit
Barge moment of inertia (I_B)	1.9800E+8	kg·m²
Tower Moment of inertia (I_T)	2.8300E+9	kg·m²
Barge center of mass distance from point O (L_B)	0.2818	m
Tower center of mass distance from point O (L_T)	64.0000	m
Barge mass (m_B)	5.4520E+6	kg
Tower set total mass (m_T)	5.5598E+5	kg
Barge spring constant (k_B)	1.7800E+9	N·m/rad
Tower spring constant (k_T)	1.2900E+10	N·m/rad
Gravitational acceleration (g)	9.7800	m/s²

Hamilton's Principle is used to derive the equations of motion of the FWOT:

$$\delta \int_{t_1}^{t_2} [T - (\mathrm{U} - \mathrm{W})]\mathrm{dt} = 0\,; \tag{1}$$

where δ is the variational operator, T is the kinetic energy, U the elastic potential energy, W the work done by the external loads, and t_1 and t_2 are initial and final times.

The kinetic and elastic potential energy expressions are, respectively, equal to:

$$T = \frac{1}{2} I_B \dot{\theta}_B^2 + \frac{1}{2} I_T \dot{\theta}_T^2; \tag{2}$$

$$U = \tfrac{1}{2} k_B \theta_B^2 + \tfrac{1}{2} k_T (\theta_B - \theta_T)^2; \tag{3}$$

where I_B and I_T are, respectively, the central moments of inertia of the barge and the tower.

The work done by the weight of tower and barge is given by:

$$W = m_B g\, L_B (1 - \cos(\theta_B)) - m_T g L_T (1 - \cos(\theta_T)); \tag{4}$$

where g is the gravitational acceleration.

The equations of motion are obtained by substituting eqs. (2)-(4) into eq. (1) and by applying the variational techniques, which results in the following set of two nonlinear Lagrange's equations:

$$I_B \ddot{\theta}_B + k_B \theta_B - k_T (\theta_T - \theta_B) + m_B g L_B \sin(\theta_B) = 0; \tag{5}$$

$$I_T \ddot{\theta}_T^2 + k_T (\theta_T - \theta_B) - m_T g L_T (\sin(\theta_T)) = 0. \tag{6}$$

As a first nonlinear approximated analysis, it is common to expand the sine terms in Taylor's series up to third degree terms, resulting in the following approximated equations of motion:

$$I_B\ddot{\theta}_B + k_B\theta_B + k_T(\theta_T - \theta_B) + m_B g L_B - \frac{1}{6} m_B g L_B \theta_B^3 = 0; \tag{7}$$

$$I_T\ddot{\theta}_T + k_T(\theta_T - \theta_B) - m_T g L_T + \frac{1}{6} m_T g L_T \theta_T^3 = 0. \tag{8}$$

3 Modal Analysis

The underlying linear problem corresponded to eqs. (7) and (8) and the use of the parameters listed on Table 1 result in the following natural frequencies of vibration for the FWOT: ω_{01}=0.5273 rad/s (0.0839 Hz) and ω_{02} = 3.4028 rad/s (0.5416 Hz). In order to avoid external resonance, the natural frequencies of the FOWT must be located out of the typical wave frequency range, which varies according to Bachynski [8] from 0.04 to 0.25 Hz. Thus, an external resonance could happen in the vicinity of the first natural frequency of the FWOT.

The nonlinear modal analysis performed in this work uses the invariant manifold approach proposed by Shaw and Pierre [9]. The nonlinear normal mode, according to the invariant manifold definition, corresponds to a motion bounded by a hypersurface in the system phase space. This surface is tangent, at the equilibrium position, to the eigenspace formed by the linear modes of the linearized underlying problem and is given by the solution of the following nonlinear partial differential equations system (Pescheck et al. [10]):

$$Q_2(u,v) = \frac{\partial P_2(u,v)}{\partial u} v + \frac{\partial P_2(u,v)}{\partial v} f_1\big(u, P_2(u,v), v, Q_2(u,v)\big)\,; \tag{9}$$

$$f_2\big(u, P_2(u,v), v, Q_2(u,v)\big) = \frac{\partial Q_2(u,v)}{\partial u} v + \frac{\partial Q_i(u,v)}{\partial v} f_1\big(u, P_2(u,v), v, Q_2(u,v)\big). \tag{10}$$

Equations (9) and (10) govern the motion corresponding to a single nonlinear mode, which can be parameterized by the displacement-velocity coordinates pair of a single degree-of-freedom of the system, (*u, v*) which is called the master pair. In this work $\theta_B = u$ and $\dot{\theta}_B = v$ are taken as the master pair while the remaining degrees-of-freedom, i. e., θ_T and $\dot{\theta}_T$, called slave coordinates, are related to the master pair via constraint equations $\theta_T = P_2$ and $\dot{\theta}_T = Q_2$. The f_1 and f_2 functions are obtained by rewriting the Lagrange's eqs. (7) and (8) as Hamilton's equations, and by using the master and slave coordinates with the parameters values listed on Table 1, which results:

$$\dot{\theta}_B = v; \quad \dot{v} = f_1(u,v) = -7.4217u + 6.5151P_2(u,v) - 0.0013u^3\,; \tag{11}$$

$$\dot{\theta}_B = Q_2(\dot{u},v); \quad Q_2(u,v) = f_2(u,v) - 4.4353P_2(u,v) + 4.5583u - 0.0205P_2^3(u,v). \tag{12}$$

The constraint functions (P_2 and Q_2) determine the invariant manifold geometry for a given NNM and are the solution of eqs. (9) and (10), which in general, do not have an exact closed form solution, except in the presence of certain conditions of symmetry (Pescheck et al., [10]). Thus, the asymptotical approximation method proposed by Shaw and Pierre [9] can be used in this case. This is done by assuming a cubic polynomial solution due to the type of non-linearity linearities present in eqs (11) and (12), and analytically solving the system of equations defined by eqs. (9) and (10). This results in two solutions for the coefficients of the power series assumed as constraint functions, one for each NNM. Replacing the generalized coordinates of the master and the slave pairs into the equations of motion, the following one-degree-of-freedom nonlinear modal oscillator is obtained for the first and second NNMs, respectively:

$$\ddot{u} + 0.2781u + 0.0161u^3 - 0.0108u\dot{u}^2 = 0\,; \tag{13}$$

$$\ddot{u} + 11.5790u + 0.0015u^3 + 0.0002u\dot{u}^2 = 0. \tag{14}$$

Those modal oscillators can be used to describe the behavior of a specific motion corresponding to a NNM, identifying important nonlinear dynamic phenomena in free and forced vibration. They correspond, also, to a reduction in the order of the problem, which facilitates the nonlinear vibration study of the system.

The domain of validity of the asymptotical method is not known a priori, but can be determined by the comparison between the modal oscillators results and the numerical integration of the original equations of motion, identified as the reference solution in Fig. 2 where the frequency-amplitude relations for both modes are presented. The frequency-amplitude relations are obtained using the harmonic balance method with an approximated solution given by the first cosine harmonic, i. e., $u = X^* \cos(\omega t)$. The dimensionless parameter Ω=ω/ω_{0i} is used as the horizontal axes for Fig. 2. The modal transformation between the physical and modal coordinates is performed by using the method proposed by Shaw and Pierre [11]. The solution using the modal oscillators concurs with numerical solution up to amplitudes of 1.0 rad for both modes. The results from Fig. 2 indicate a hardening behavior for both modes. The hardening behavior is confirmed by the frequency-energy (Π -Ω) dependence, another exclusive nonlinear feature, and can be observed in Fig. 3 where a semi-log plot is used.

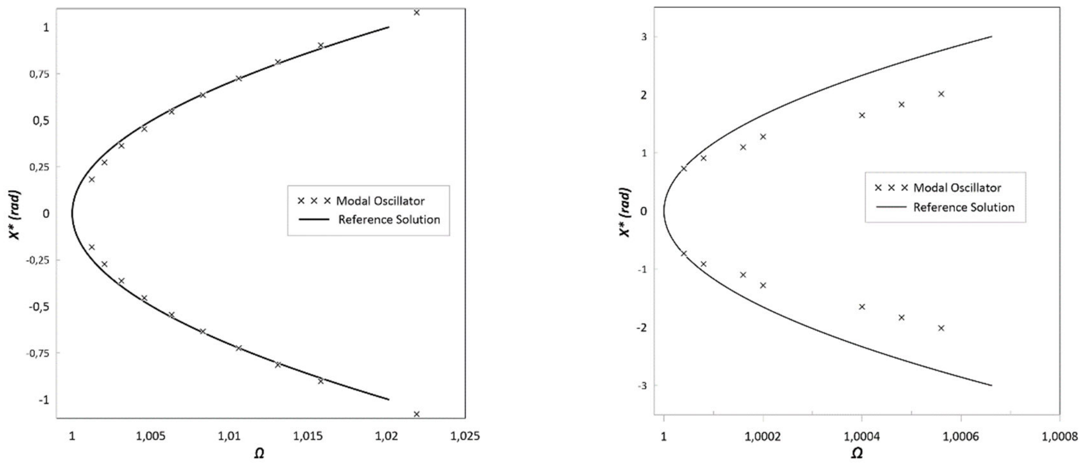

(a) (b)

Figure 2. Frequency-amplitude relations: (a) First NNM, and (b) second NNM.

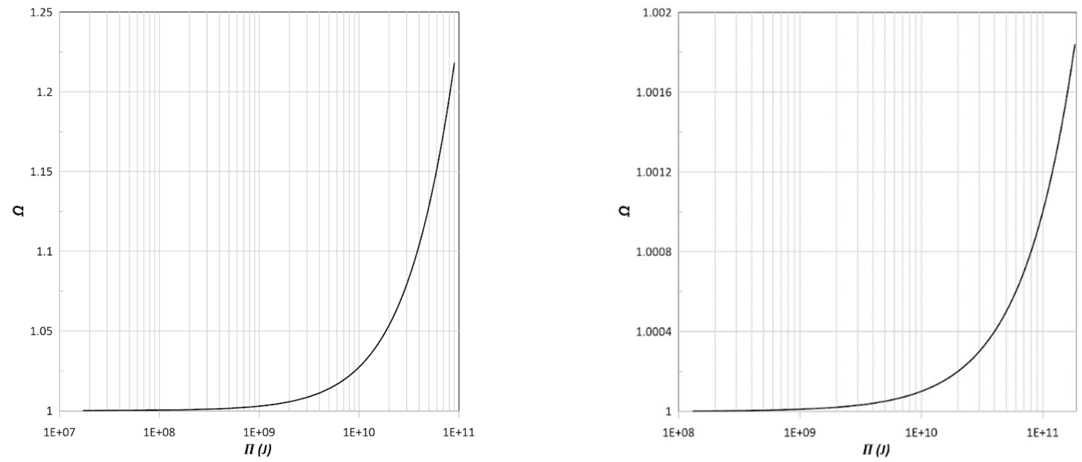

(a) (b)

Figure 3: Frequency-energy curves: (a) First NNM, and (b) Second NNM.

4 Forced Vibration

As the resonant response of a structural system occurs at the vicinity of NNM motion (Vakakis et al., [12]), the modal oscillators given by eqs. (13) and (14) can provide useful information about the forced oscillations of the FWOT. As a preliminary study an external harmonic moment of amplitude equal to M and frequency ω is used here. Since this study focus on permanent regime, a small viscous damping (ξ coefficient) is included, resulting in the following forced-damped modal oscillator equations:

$$\ddot{u} + 0.2781u + 1.0546\xi\dot{u} + 0.0161u^3 - 0.0108u\dot{u}^2 = 0.2378\Gamma\sin(\omega t); \tag{15}$$

$$\ddot{u} + 11.5790u + 6.8056\xi\dot{u} + 0.0015u^3 + 0.0002u\dot{u}^2 = 0.2378\Gamma\sin(\omega t); \tag{16}$$

where Γ is included to facilitate parametric studies and its equal to M/M_0, where M_0 is the moment caused by the weight of the displaced volume of water corresponded to the motion of the barge draft.

The resonance curves can be obtained using the harmonic balance method; the effect of the external moment magnitude and damping for the 1st NNM are shown (results for the 2nd NNM are not shown because they are very similar to the 1st one), respectively, in Fig. 4 (a) and (b) using a dimensionless frequency parameter defined as $\Omega=\omega/\omega_{0i}$. From Fig. 4 it is possible to observe both jump and hysteresis phenomena, indicating that the forced response of FOWT is bistable, with two possible amplitudes of motion for each frequency, for some set of damping factor and amplitude of external moment values. This is due to two saddle-node bifurcations (Points P_1 and P_2 in Fig 4 (b)) separating the stable and unstable branches along the nonlinear resonance curves. The jump is very sensitive to the damping factor ξ, being reduced (or even disappearing) with increasing damping factor as one can see from Fig. 4 (b). On the other hand, the influence of a decreasing force magnitude is of less significance, although its action is noted in reducing the width of the resonance curve as can be observed from the plots of Fig. 4 (a).

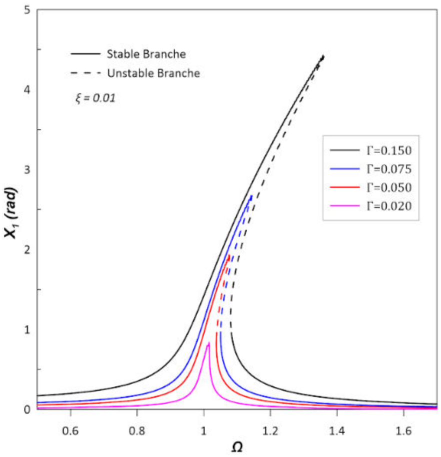

(a)

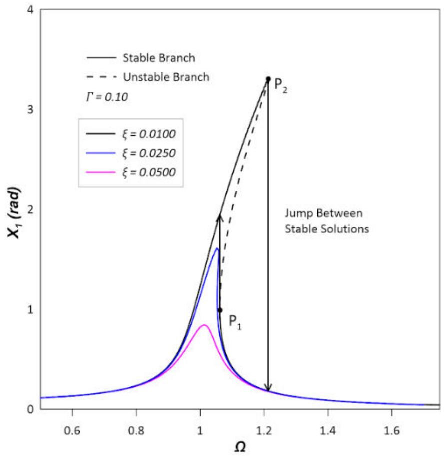

(b)

Figure 4. Resonances curves of the first NNM: (a) effect of Γ, and (b) effect of ξ.

A similar jump phenomenon can be also noted when the frequency of the excitation is held fixed while the amplitude of excitation is varied slowly, as it is illustrated by the amplitude-response curves shown in Fig. 5. Again, the conclusions from Fig. 5 (b) analyis reassure the bold influence of damping in eliminating the coexistence of multiple solutions in the FOWT forced vibration response. Also, the Fig. 5 (a) indicates that bifurcations existance is greatly affected by the excitation frequencies values.

The stability domain of the solutions associated to the forced modal oscillators can be mapped in the space of the system's parameters (Ω, X^*,ξ) using the Mathieu's chart (Jordan and Smith, [13]). The Mathieu's charts for selected values of ξ are shown in Fig. 6 for the 1st NNMs. Again, the results make clear the influence of damping in the resonance response of the FWOT. The two stable regions for the a given Ω value in Fig. 6 confirms the coexistence of bistable periodic solutions. This behavior is clearly identified by the two limit cycles attractors presented in the phase-portrait shown in Fig. 7, which are obtained by using ξ=0.0100; Γ=0.2000 and Ω=1.1500 for the numerical integration of eq. (15).

5 Conclusions

According to the results of this work it is possible to obtain important features of the nonlinear dynamic behavior of a barge-type FWOT using the nonlinear normal modes theory. The invariant manifold definition and the asymptotical method used here were important tools to obtain analytical reduced order models which simplify the analysis of the system nonlinear response. Some exclusively nonlinear phenomena were observed for the examples studied here such as: frequency-amplitude and energy-amplitude dependences and, unstable and bistable solutions. A good agreement between the numerical integrations of the FOWT equations of motion and nonlinear modal oscillators was found to rotations up to 1 rad. The barge FOWT studied here presents a hardening behavior when vibrating in both the 1st and 2nd NNMs. The one-degree-of-freedom forced modal oscillators enable a parametric study of FOWT external excitation and the identification of important nonlinear features, such as backbone curves, jump phenomena, hysteresis, saddle-node bifurcations, bistable and, unstable solutions. Such phenomena, may lead to jumps between the coexisting solutions in an evolving dynamic environment which can be very harmful to the Barge FOWT structure. The analytically derived reduced order model allows the use of Mathieu's chart to map the stability of the solutions in the entire space formed by the main parameters of the problem: damping ratio, external load amplitude and frequency. Among those three parameters, damping ratio has the most prominent effect on the nonlinear dynamic response of the FWOT. Those features are of great value to the offshore engineers in the predesign cycles of such FWOT structures.

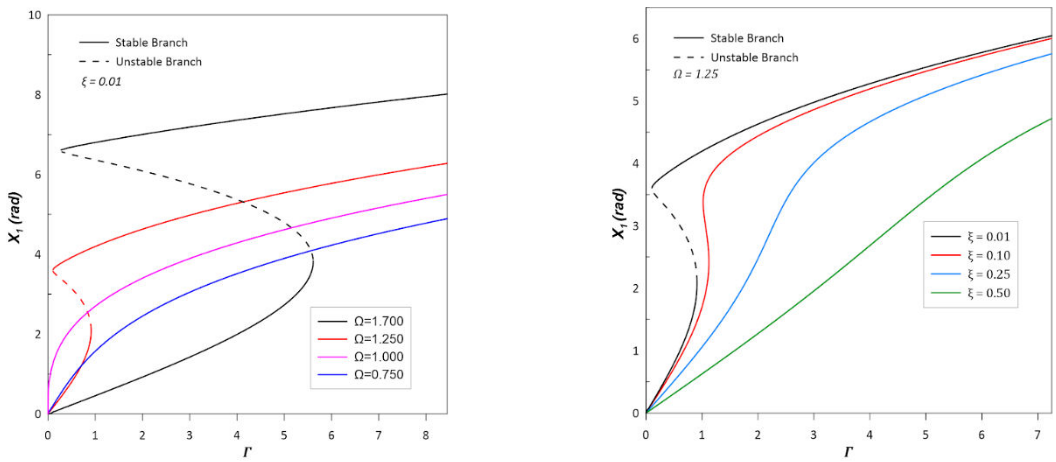

(a) (b)

Figure 5. Amplitude responses of the first NNM: (a) effect of Ω, and (b) effect of ξ.

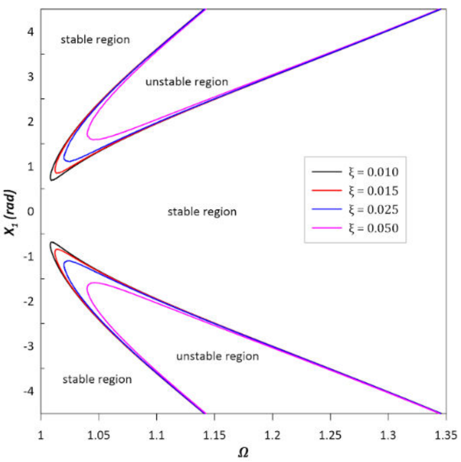

(a)

Figure 6. Mathieu's stability chart for the First NNM.

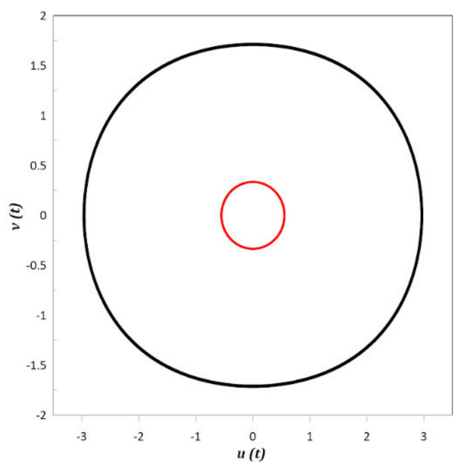

(b)

Figure 7. Limits cycles for the 1st NNM (ξ=0.0100; Γ=0.2000 and Ω=1.1500).

This is a work in progress, further work will consider the effects of a passive controller upon the linear and nonlinear dynamics of the barge-type FWOT and also to perform geometrical parametric studies of both wind tower and barge platform.

Acknowledgements. The authors would like to thank the Programa de Pós-Graduação em Engenharia de Construção Civil (PPGECC/UFPR) e o Centro de Estudos em Engenharia Civil (CESEC/ UFPR) for their support of this research

Authorship statement. The authors hereby confirm that they are the sole liable persons responsible for the authorship of this work, and that all material that has been herein included as part of the present paper is either the property (and authorship) of the authors, or has the permission of the owners to be included here.

References

[1] K. Ohlenforst *et al.*, "GLOBAL WIND REPORT 2018," 2019. Accessed: Aug. 12, 2020. [Online]. Available: www.gwec.net.

[2] S. Sarkar and B. Fitzgerald, "Vibration control of spar-type floating offshore wind turbine towers using a tuned mass-damper-inerter," *Structural Control and Health Monitoring*, vol. 27, no. 1, pp. 1–23, 2020, doi: 10.1002/stc.2471.

[3] H. Zuo, K. Bi, and H. Hao, "A state-of-the-art review on the vibration mitigation of wind turbines," *Renewable and Sustainable Energy Reviews*, vol. 121, p. 19, 2020, doi: 10.1016/j.rser.2020.109710.

[4] E. Gavassoni, P. Batista Gonçalves, D. de Mesquita Roehl, P. B. Gonçalves, and D. de M. Roehl, "Nonlinear vibration modes of an offshore articulated tower," *Ocean Engineering*, vol. 109, pp. 226–242, Nov. 2015, doi: 10.1016/j.oceaneng.2015.08.028.

[5] J. M. Jonkman, "Dynamics modeling and loads analysis of an offshore floating wind turbine," *National Renewable Energy Laboratory NREL/TP-500-41958*, vol. 68, no. November, p. 233, 2007, [Online]. Available: http://www.nrel.gov/docs/fy08osti/41958.pdf.

[6] J. Jonkman, S. Butterfield, W. Musial, and G. Scott, "Definition of a 5-MW Reference Wind Turbine for Offshore System Development, NREL Technical Report No. TP-500-38060," *NREL*, no. February, Feb. 2009, doi: 10.2172/947422.

[7] E. M. He, Y. Q. Hu, and Y. Zhang, "Optimization design of tuned mass damper for vibration suppression of a barge-type offshore floating wind turbine," *Proceedings of the Institution of Mechanical Engineers Part M: Journal of Engineering for the Maritime Environment*, vol. 231, no. 1, pp. 302–315, 2017, doi: 10.1177/1475090216642466.

[8] E. E. Bachynski, "Fixed and Floating Offshore Wind Turbine Support Structures," *Offshore Wind Energy Technology*. John Wiley & Sons, pp. 103–142, 2018, doi: 10.1002/9781119097808.ch4.

[9] S. Shaw and C. Pierre, "Non-linear normal modes and invariant manifolds To cite this version : HAL Id : hal-01310674," *Journal of Sound and Vibration*, vol. 150, no. 1, pp. 170–173, 1991.

[10] E. Pescheck *et al.*, "Non-linear modal analysis of structural systems using multi-mode invariant manifolds," *Nonlinear Dynamics*, vol. 25, no. 734, pp. 183–205, 1994, doi: 10.2514/6.1994-1672.

[11] S. Shaw *et al.*, "Normal Modes for Non-Linear Vibratory Systems To cite this version : HAL Id : hal-01544500 NORMAL MODES FOR NO : N-LINEAR," *Journal of Sound and Vibration*, vol. 164, no. 1, pp. 85–124, 1993.

[12] A. F. Vakakis, L. I. Manevitch, Y. V. Mikhlin, V. N. Pilipchuk, and A. A. Zevin, "Normal Modes and Localization in," p. 552, 1996.

[13] D. W. Jordan and P. Smith, *Nonlinear ordinary differential equations*, Fourth. Oxford University Press, 2017.